Identification of particulate materials by correlation analysis using a microscopic laser induced breakdown spectrometer

JAAS

Full Paper

I. B. Gornushkin, A. Ruíz-Medina,† J. M. Anzano,‡ B. W. Smith and J. D. Winefordner*

Department of Chemistry, PO Box 117200, University of Florida, Gainesville, FL 32611, USA

Received 16th December 1999, Accepted 21st March 2000
Published on the Web 9th May 2000

The goal of this work was the instant identification of particulate geological materials by comparison with spectral libraries stored in a computer. The libraries consisted of representative spectra from different groups of powdered samples. Special attention was paid to identification of particles with very similar chemical composition, such as certain iron ores. Chemical speciation analysis was also carried out. Iron and iron oxides were shown to be reliably identified using statistical correlation methods. Both linear and rank correlations were applied. Both correlation methods yielded probabilities of correct identification close to unity for almost all studied samples. This technique should have applications in the metallurgical, mining, and semiconductor industries, and in medical, environmental and forensic sciences.

Introduction

The rapid identification of different materials is a new interesting application of LIBS. Sattmann *et al.*[1] explored the potential of LIBS for polymer identification using artificial neural networks. The laser plasma was produced on the polymer target by two separated pulses of 6 µs from a Nd:YAG laser and the spectrum was detected with a photodiode array in a 70 nm spectral window. The variables for the neural networks were H_β, C, C_2 and Cl spectral line intensities, intensity ratios and intensity *vs.* background ratios. The samples were high- and low-density polyethylene, polyvinyl chloride, polyethylene terephthalate, and polypropylene. The identification accuracy was between 90 and 100%, depending on polymer type. Devos *et al.*[2] used LA-ICP-MS for authentication of antique silver objects. A special cell was designed to be placed upon the entire object for removing a microscopic amount of the sample and transporting it into the ICP-MS. The analytes Zn, Cd, Sn, Sb, Au, Pb and Bi were measured as indicators of the age of the objects. The method was shown to be sufficiently precise and accurate to allow "before/after" (1850) dating of antique silverware. The main advantages over wet techniques was the virtual non-destructiveness and analysis speed.

In a previous paper,[3] we have shown that simple statistical correlation methods, such as linear and rank correlations, can also be successfully applied to identification of solid samples. A nearly 100% reliable identification of different brands of steel and cast iron was achieved. In contrast to other correlation procedures, like wavelets[4] or neural networks,[5] which require preliminary network training or search for an adequate wavelet algorithm, linear and rank correlations are fast and straightforward. Their success is based on the use of thousands of data points (pixels) representing the sample spectrum in a relatively large spectral window.

Another application of this approach is for the rapid identification of particulate material. Analysis and characterization of particles is important in many fields. In mineralogy, reliable classification of grain polycrystalline samples is a routine task for analytical laboratories.[5] Thousands of samples have to be quickly classified in a qualitative way, *i.e.*, whether they contain certain minerals or whether they can be attributed to a certain known mineralogical group. The usual technique for such identification is energy-dispersive X-ray spectrometry (EDX).[6] Ruisanchez *et al.*[5] used EDX for classification of individual grains (≈200 µm in size) taken from large matrices. The mineral types into which particulates had to be classified were pyrrhotite, pyrite, chalcopyrite, *etc.* A 100% correct classification was achieved using the artificial neural network method. Another important field is the analysis, both qualitative and quantitative, of aerosols and suspensions. Chin *et al.*[7] reported on the direct analysis of air-borne particulate matter collected on a membrane filter using LA-ICP-MS. Hahn[8] used LIBS for sizing and elemental analysis of aerosol particles directly in the air. A novel two-part calibration scheme was developed which established the LIBS system response to a known mass concentration ($\mu g\, m^{-3}$) and a known discrete particle mass. The characteristic plasma volume was then determined, and the overall procedure allowed for quantitative analysis of the mass and elemental composition of individual, sub-micrometer to micrometer-sized aerosol particles. Saito *et al.*[9] developed LIBS instrumentation with an acoustic sensor for detection of microparticles in pure water. Polystyrene and silica partcles were successfully detected down to a size of 0.04 µm. Cheung *et al.*[10] used LIBS for analysis of biological particulates. The Na and K contents were determined in single human erythrocytes. In forensic science, rapid identification of particulate gun powder residues, left on a crime scene or on a person's skin, would be of a great importance in tracing cases where guns were used. Watling *et al.*[11] have reported on the use of LA-ICP-MS for fingerprinting at crime scenes. Several tens of glass and steel samples, which frequently occur as physical evidence, were examined. Specimens of about 50 µm were analyzed. Their spectra were compared by direct overlay or by using interpretive software which facilitated the simultaneous inter-comparison of three elements (ternary plots). Robust analytical procedures were developed which reliably discriminated both steel and glass samples.

In this paper, we demonstrate the application of the correlation methodology to the analysis of a variety of particulate materials.

†Present address: Departamento de Química Física y Analítica, Facultad de Ciencias Experimentales, Universidad de Jaén, Paraje las Lagunillas s/n, 23071, Jaén, Spain.
‡Present address: Departamento de Química Analítica Facultad de Veterinaria, Universidad de Zaragoza, Miguel Servet, 177, 50013 Zaragoza, Spain.

Experimental

Spectrometer

The microscopic LIB spectrometer, developed in our laboratory, is described elsewhere.[3] Briefly, it consisted of a compact Nd : YAG laser (Model MK-367, Kigre, Inc., USA) which is attached to a modified microscope (Zeiss, Germany). The laser output is aligned with the microscope optical system using a dichroic mirror placed inside the microscope enclosure. The mirror reflects 99% of the laser radiation at 1064 nm and transmits visible light coming from the illuminated particulate sample. A magnified image of the sample is monitored with a TV camera (VCC 3700, Sanyo Electric Inc., Compton, CA) mounted on the top of the microscope and connected to a 10 inch TV monitor (CT-1020-M, Panasonic). Microscope magnification can be varied with a set of objectives placed in a rotatable amount. For the present work, we used the 10 × objective (total magnification 500 ×) with a working distance of 5 mm between the objective tip and the sample surface. With the 10 × working objective, the laser is focused to a ≈20 µm diameter spot on the particle surface providing an irradiance of $\approx 10^{12}$ W cm^{-2}. The laser and the spectrometer are synchronized by a trigger pulse from a home-made compact pulse generator working either in a single pulse mode or at a 0.2 Hz repetition rate.

The radiation from the laser spark is collected with a bifurcated optical fiber connected to a dual-channel Ocean Optics mini-spectrometer (SD2000, Ocean Optics, Inc., Dunedin, FL, USA). The spectrometer has the following characteristics: channel one, 230–310 nm spectral range, 3600 mm^{-1} holographic grating, 25 µm slit, 0.16 nm spectral resolution, 2048 pixel linear CCD array; and channel two, 200–850 nm spectral range, 600 mm^{-1} grating blazed at 400 nm, 25 µm slit, 1.3 nm spectral resolution, 2048 pixel linear CCD array. The spectrometer is driven from a laptop computer *via* a DAQCard-700 interface (National Instruments, USA).

Samples

The samples were powdered materials placed on a double-sided tape stuck to a microscope slide. The powders were scattered over the tape surface so that single particles, separated from each other by a distance of several particle diameters, could be distinctly seen. Four iron ore NIST standards were used along with a number of iron ore samples obtained from the Cleveland Cliffs mining company. For the speciation study, powders of Fe, Fe_2O_3 and Fe_3O_4 (all from Fisher Scientific) were used. Particle sizes in all samples ranged between 40 µm and 200 µm.

LIBS libraries

Three LIBS libraries were compiled for identification of three groups of materials: NIST standards, natural ore samples, and iron and iron oxides. The library spectrum of a particulate material was obtained by inducing the laser spark on 10 random particles and averaging their emission spectra. Only the high resolution spectrometer channel (230–310 nm) was used because the most characteristic spectra from all samples appeared in this spectral window. All libraries were stored in a computer and could be chosen by the operator prior to analysis.

Software

A program for correlation analysis was developed using Visual Basic 6.0 and the LabView drivers supplied with the Ocean Optics spectrometer. A detailed description of the program can be found elsewhere.[3] In brief, the software offers the following options to an operator: (i) choice of appropriate experimental parameters (integration time, trigger type, spectrometer channel, number of spectra to average, library file); (ii) pre-treatment of the spectrum (reduction in the spectral range, correction for continuous plasma background); and (iii) selection of a correlation method (linear or rank). The computer calculates all mutual correlation coefficients between the current spectrum and all library spectra. The correlation plot corresponding to the maximum correlation coefficient is displayed along with the statistical parameters (correlation coefficients, errors, probabilities) and the name of the compound which is identified with the highest correlation probability. If desired, the correlation can be repeated with the use of another correlation method. The output data are saved and stored in a computer.

Results and discussion

Laser ablation on a particle is quite different from that on a surface of a bulk solid if the particle size is on the order of the laser beam diameter. For particles, the emission spectrum and ablated mass are affected by particle size and particle/environment interface, whereas for ablation on a solid surface, bulk material properties (thermal conductivity, heat capacity, *etc.*) are of primary importance.[12] We investigated how the particle size affected the emission spectrum on the example of SiC particulate of certified sizes ranging from 12 µm to 1000 µm (AGSCO corp., USA). The available particle sizes were 12, 16, 50, 115, 210, 640, and 1000 µm. The spectral line intensities did not show any dependence upon the particle size for particles larger than 50 µm. For smaller particles ($\leqslant$16 µm), the spectral line intensities gradually decreased indicating that only a fraction of the laser radiation efficiently vaporizes the particle and the rest of the laser radiation interacts only with the substrate material. The slight change in the relative C *vs.* Si line intensities was caused by a slight vaporization of the carbon-containing substrate. It is important for a robust correlation that the ratio of line intensities to background remains the same for the same material. Therefore, only particles larger than ≈20 µm (approximately focused laser beam diameter) should be used.

The correlation methodology was first applied to iron ore NIST standards of well known composition (Table 1). Spectra from the standards, shown in Fig. 1(a), were obtained using a 10-fold attenuating filter to prevent saturation of the detector. Visual examination shows minimal differences in the spectra. Indeed, with the exception of NIST 692, which contained twice the concentration of silica, the composition of the samples in terms of major constituents (>1%), is very similar. Although the Mn and Al content also varied between the samples, our spectrometer was insensitive to these variations, especially when the 10-fold attenuating filter was used. Silicon lines were also not distinct in the spectra, being 10-times attenuated. This

Table 1 Composition (%) of NIST and Cleveland Cliffs iron ore samples

Sample	Fe	SiO_2	Al_2O_3	Mn
NIST ores				
27f	65.97	4.71	0.82	0.0085
690	66.85	3.71	0.18	0.18
692	59.58	10.14	1.41	0.36
693	65.11	3.87	1.02	0.070
Cleveland ores[a]				
2765 B	63.3	2.56	nc[b]	2.57
2805 B	60.8	7.03	nc	2.50
2808 G	61.6	4.99	nc	2.75
3274 B	60.5	9.43	nc	1.53
S1	68.7	1.02	nc	0.42
S2	65.4	2.93	nc	2.04

[a]Analyzed by digestion-ICP-OES. [b]nc = not certified.

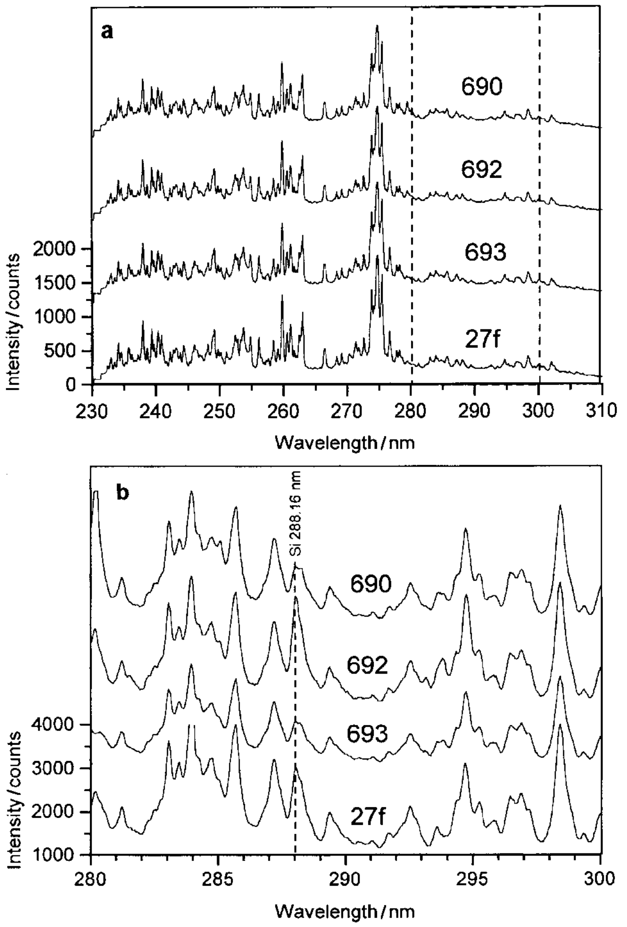

Fig. 1 Spectra from NIST iron ores: (a) obtained in the entire spectral range using a 1.0 neutral density filter; (b) obtained in the reduced spectral range without a filter.

made the spectra almost identical suggesting the need to use powerful statistical methods for detection of differences.

Because the emission spectra consist of 2048 points (pixels), enough statistical information is available to permit the use of simple correlation methods like linear correlation and non-parametric rank correlation. Linear correlation measures the association between variables with a linear correlation coefficient, r, expressed in the following form:

$$r = \frac{\sum_i (x_i - \bar{x})(y_i - \bar{y})}{\sqrt{\sum_i (x_i - \bar{x})^2}\sqrt{\sum_i (y_i - \bar{y})^2}} \tag{1}$$

where $\bar{x}$ is the mean of x_i values, and $\bar{y}$ is the mean of y_i values. The value of r lies between -1 and 1; $r=1$ corresponds to complete positive correlation when the data points lie on a perfect straight line with positive slope, with x and y increasing together. The "goodness" of the correlation can be estimated from:[13]

$$\alpha = erfc\left(\frac{|r|\sqrt{N}}{\sqrt{2}}\right), \quad erfc(x) = \frac{2}{\pi}\int_x^{\infty} e^{-t^2}dt \tag{2}$$

where α denotes the correlation significance, $erfc(x)$ is the complementary error function, and N is the number of data points. A small value of α indicates that two variables are significantly correlated. Press *et al.*[13] pointed out, however, that the linear correlation coefficient r is a poor statistic for deciding whether an observed correlation is statistically significant or not because r is ignorant of the individual distributions of x and y. This may be important in our case where we compare fluctuating single-shot spectra (x values with different distributions) with stable library spectra (y values). In this situation, non-parametric rank correlation, where the x_i and y_i distributions are known *a priori*, is likely to be more robust. The equation for non-parametric correlation is the same as eqn. (1) but now the values of x and y are replaced by their corresponding ranks:

$$r = \frac{\sum_i (R_i - \bar{R})(S_i - \bar{S})}{\sqrt{\sum_i (R_i - \bar{R})^2}\sqrt{\sum_i (S_i - \bar{S})^2}} \tag{3}$$

where R_i is the rank of x_i among the other x values, S_i is the rank of y_i among the other y values, $\bar{R}$ and $\bar{S}$ are the means of the ranks. As before, x_i (or its corresponding rank R_i) stands for the intensity of light detected by pixel i in the probe (or current) spectrum, whereas y_i (or its corresponding rank S_i) stands for the intensity at the same pixel i of the stored library spectrum which is correlated with the current spectrum. The ranks are numbers 1,2,3,...,N, where N is a total number of data points (or pixels in our detector, 2048), which replace the true values of x and y in accordance with their magnitudes. For example, the most intense pixel in a spectrum is assigned the number 2048, the least intense, the number 1, *i.e.*, the higher the intensity, the higher the rank. Hence, the resulting list of numbers is drawn from a perfectly known distribution function, namely uniformly from the integers between 1 and N. It is important to emphasize that if a correlation is proven non-parametrically, then it really exists.[13]

We applied both correlation methods to the NIST iron ores with the goal of reliable identification of single particles which belong to different ores. In this case, a single shot is the only sampling event; therefore, spectra were not averaged and each single-shot spectrum was used to correlate with the NIST iron ore spectral library (10 particle averages). Typical correlation plots for the two correlation methods are shown in Fig. 2. Shown in Fig. 3 are the averaged (over 10 laser shots) linear and rank correlation coefficients. One can see from Fig. 3 that the rank correlation provides about the same separation between mean correlation coefficients.

Besides the apparent differences in correlation coefficients, strict statistical criteria must be used in order to quantify the level of significance of these differences. To do this, we applied a simple Student's t-test. The values for the Student's t were calculated differently depending on whether the two distributions had the same or different variances. To check this, an F-test was applied (F denoting the ratio of the variances). If the calculated significance of F did not exceed 0.1, the difference in variances was considered as significant and t was calculated in a slightly different way than in the case where the distributions had the same variances.[13] On the basis of these t-values, the probabilities that two distributions of correlation coefficients had different means were calculated. The first lines in Table 2 show the results of these calculations. The diagonal elements in Table 2 correspond to the correlation of the sample with itself, all exhibiting a zero probability of difference. All the probabilities given in the table as unity differ from unity by negligibly small numbers, less than 10^{-8}.

As seen in Table 2 (first line), both correlations show very high ($>90\%$) probabilities of correct identification, except for a few cases. For example, for the linear correlation, sample 690 is somewhat confused with samples 693 (0.89 probability), 692 (0.54), and 27f (0.72). The rank correlation shows a higher probability of identification for this particular sample but gives lower values for another one (692 *vs.* 690 and 692 *vs.* 27f).

Here, it is important to recall that the spectra were recorded using a 1.0 neutral density filter (10-fold attenuation) placed in front of the spectrometer. The filter was used in order to avoid saturation of the detector at some strong iron lines (for example, Fe II 275 nm); however, some important information

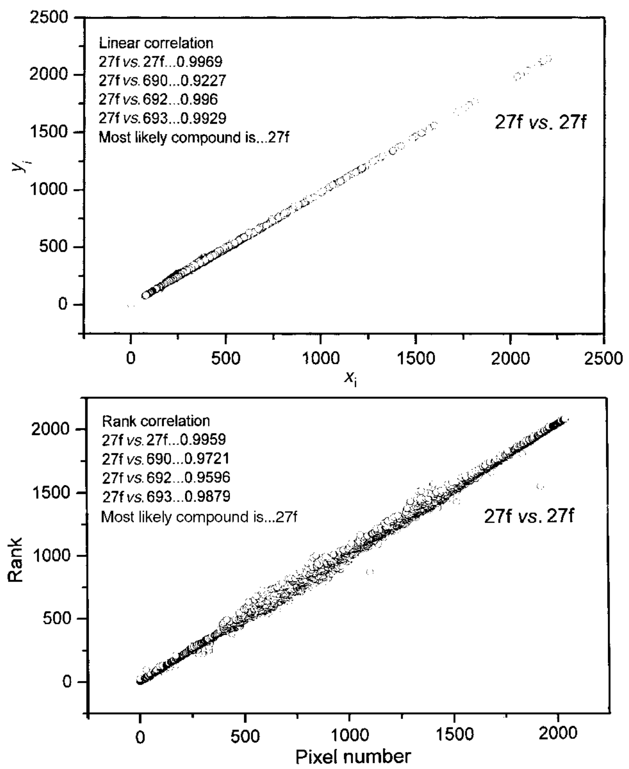

Fig. 2 Linear and rank correlation plots for the NIST 27f (current) *vs.* NIST 27f (library). The NIST 27f spectrum was acquired with the spectrometer and correlated against all library spectra stored in the computer. The corresponding correlation coefficients are printed in the plot box.

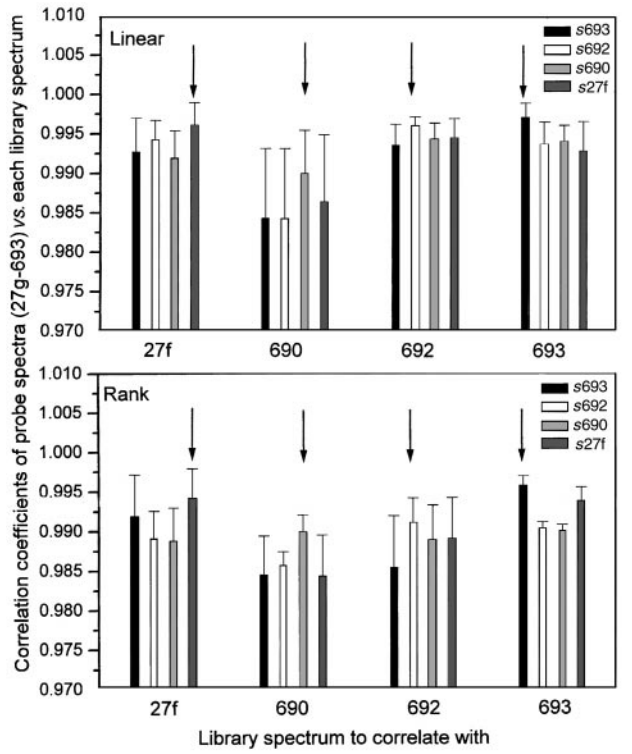

Fig. 3 Linear and rank correlation coefficients for the four NIST iron ores. A 10-fold attenuation filter and a large spectral window of 230–310 nm were used. Arrows indicate samples which show maximum correlation coefficients. If identification is correct, the indicated samples are the same as the library spectrum shown on the *x*-axis.

for correlation was lost. The filter, in turn, decreased the instrument's sensitivity. Therefore, spectra from minor elemental constituents (like Si in NIST ore samples) did not play the same crucial role for correlation as did stronger spectral lines from the major component, iron.

In order to increase the contribution of minor constituents to the correlation analysis, we removed the filter and used a fragment of the spectrum which satisfied two conditions: (i) it contained minor constituent lines; and (ii) it did not saturate the detector. This spectral fragment window was 280–300 nm which contained the 288.16 nm silicon line as well as several iron lines. Now, differences in the intensities of silicon lines were clearly seen [Fig. 1(b)] and the probabilities of correct identification were very close to unity for all samples (see Table 2, values in parentheses). Average values of correlation coefficients are given in Fig. 4. Although their absolute values are somewhat lower than for the case when the entire spectrum was used, the separation between correlation coefficient is better (compare to Fig. 3).

Thus, despite the smaller number of variables (pixels) available for correlation, the correlation quality improved because more details, specific to each sample, were revealed. We note that the appropriate spectral range could be easily chosen or changed with the software, and no additional spectral acquisitions were necessary. The example above shows that some preliminary knowledge about the sample nature (*e.g.*, composition and concentrations of some constituents) is useful and can improve the results of correlation analysis, although not dramatically.

Surprisingly, we did not experience any difficulties when the correlation methodology was applied to naturally occurring samples, namely, iron ores obtained from the Cleveland Cliffs mining company (Table 1). The samples were expected to be less homogeneous than NIST standards and therefore to show poorer correlation for random single-shot sampling. This, however, did not occur and identification probabilities for all samples were close to unity (Table 3) even with the use of the entire spectral window (230–310 nm). This result has immediate practical implications. For the mining industry, for example, it is very important to provide a fast feedback between an analytical laboratory and a mining facility in order to prevent processing of poor quality ores. Fast on-line LIBS identification can successfully solve this problem.

Table 2 Calculated probabilities that differences in iron ore samples were detected using 10 shot-averaged library spectra; data in parentheses relate to the spectral range of 280–300 nm

Correlation type	Linear correlation with:				Rank correlation with:			
Samples	693	692	690	27f	693	692	690	27f
693	0	0.9949 (1)	0.9977 (1)	0.9938 (0.9996)	0	1 (1)	1 (1)	0.9862 (0.9374)
692	0.9815 (0.9955)	0	0.9629 (1)	0.9054 (0.9999)	0.9714 (0.9999)	0	0.7794 (1)	0.6896 (0.9998)
690	0.8946 (0.9999)	0.5428 (0.9993)	0	0.7235 (0.9999)	0.9927 (1)	0.9999 (0.9998)	0	0.9915 (0.9999)
27f	0.95 (0.9961)	0.8753 (1)	0.9916 (1)	0	0.7202 (1)	0.9947 (1)	0.9929 (1)	0

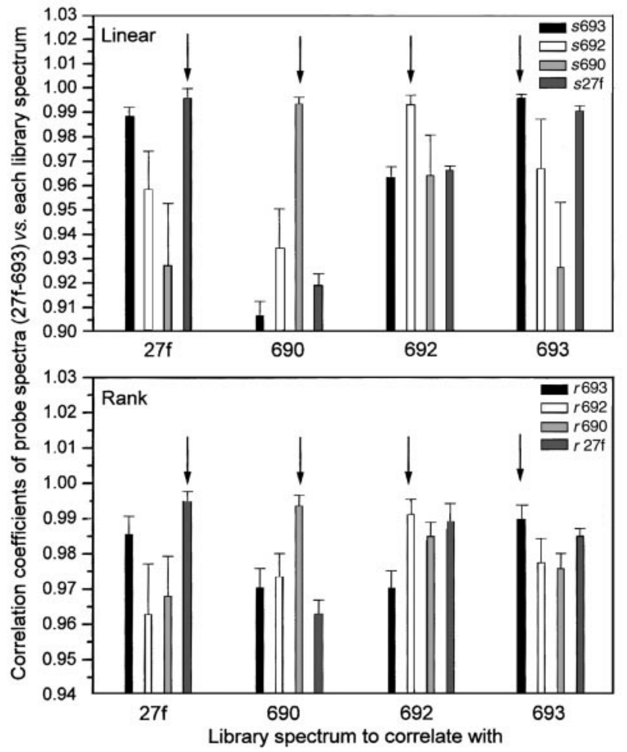

Fig. 4 Linear and rank correlation coefficients for the four NIST iron ores. No filter was used in a narrow spectral window of 280–300 nm. Arrows indicate samples which showed maximum correlation coefficients.

Table 3 Calculated probabilities that differences in Cleveland Cliffs ores were detected using 10 shot-averaged library spectra

Correlation type	Linear correlation with:					
Sample	2765	2805	2808	3274	S1	S2
2765	0	1	0.994	1	1	0.7201
2805	0.9986	0	0.9998	0.9993	0.9999	0.9914
2808	0.9523	0.9999	0	1	1	0.9195
3274	1	0.9975	1	0	0.9932	1
S1	0.9999	0.9792	1	0.9484	0	0.9999
S2	0.9099	0.999	1	1	1	0
Correlation type	Rank correlation with:					
Sample	2765	2805	2808	3274	S1	S2
2765	0	0.9681	0.9095	0.996	1	0.9195
2805	0.9923	0	0.9998	0.9997	1	0.9394
2808	0.9285	1	0	1	1	0.9409
3274	0.9999	0.999	1	0	0.992	1
S1	1	0.9974	1	0.971	0	0.9998
S2	0.8531	0.9997	0.9774	1	1	0

Finally, we evaluated the application of the correlation procedure for chemical speciation analysis. Three iron-based powdered materials were chosen: pure iron, hematite (Fe_2O_3), and magnetite (Fe_3O_4). Single-shot, single-particle spectra from these materials are shown in Fig. 5. By preliminary visual inspection of the spectra, we found that both ferric and ferrous oxides were contaminated by Mg. Therefore, the short spectral window of 230–277 nm was used for correlation in order to exclude the influence of the strong line of Mg at 280 nm. Despite the obvious similarity of the spectra (Fig. 5), the results of identification were 100% accurate (see Table 4). An exact knowledge of chemical speciation is also of great importance for the optimum processing of iron ores.

Conclusions

Several groups of iron-based particulate materials (iron ores and iron oxides) were reliably identified by using laser induced breakdown spectrometry. A compact laser induced breakdown spectrometer with microscopic sample imaging has been developed along with software which combined both data acquisition and data processing functions. Differences in spectra were detected using simple statistical linear and rank correlation methods. Both correlations yielded approximately the same results. The robustness of the technique was demonstrated by the nearly 100% reliable identification of NIST iron ores and natural iron ore samples. Also, chemical speciation of iron compounds was demonstrated. Overall, the attractive features of the technique are its simplicity, small size, low cost and a good potential for identification of various kinds of materials regardless of their aggregate state and without preliminary sample preparation. Provided that the spectral libraries for a variety of compounds are collected and stored in the computer, the analysis time is minimal, about several minutes. In the current design, based on the miniature fiber optic spectrometer, the technique has one limitation: its sensitivity is quite low and therefore spectral information from minor components (0.1–1%) is lost. However, this drawback can easily be overcome by using more sensitive detectors, like intensified CCDs. Overall, we demonstrated that the technique can have immediate application for on-line, real-

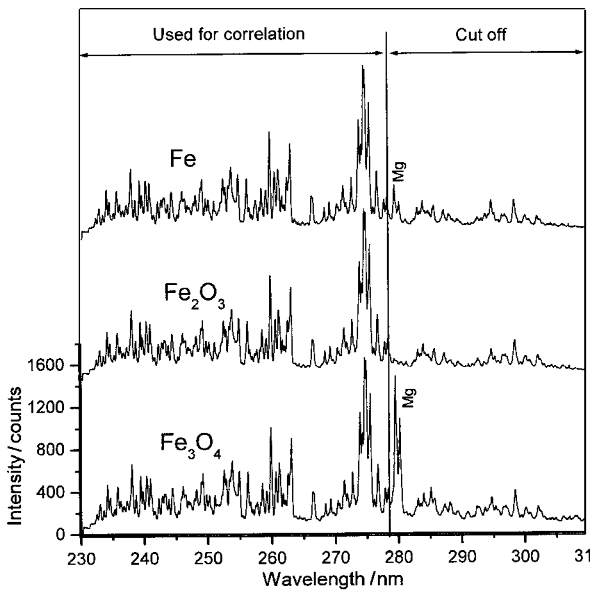

Fig. 5 Portions of iron and iron oxide spectra used for correlation. No visible differences can be detected.

Table 4 Calculated probabilities that differences in iron samples were detected using 10 shot-averaged library spectra

Correlation type	Linear correlation with:			Rank correlation with:		
Sample	Fe	Fe_2O_3	Fe_3O_4	Fe	Fe_2O_3	Fe_3O_4
Fe	0	1	1	0	1	1
Fe_2O_3	1	0	1	1	0	1
Fe_3O_4	1	1	0	1	1	0

time analysis of raw materials which is important in the mining and chemical processing industries. Potentially, it can also be applied in forensic, environmental, medical and other fields.

Acknowledgement

This work was supported by the Engineering Research Center (ERC) for Particle Science and Technology at the University of Florida, the National Science Foundation (NSF grant No. EEC 94-02989), the Industrial Partners of the ERC and the Florida Institute of Phosphate Research (FIPR 96-04-057R). We are thankful to the Cleveland Cliffs Company, Ishpeming, MI, for providing a variety of analyzed iron ore samples. A grant No. PR99 from the Spanish Education and Culture Ministry to Jesús M. Anzano is also gratefully acknowledged.

References

1 R. Sattmann, I. Mönch, H. Krause, R. Noll, S. Couris, A. Hatziapostolou, A. Mavromanolakis, C. Fotakis, E. Larrauri and R. Miguel, *Appl. Spectrosc.*, 1998, **52**, 456.
2 W. Devos, C. Moor and P. Lienemann, *J. Anal. At. Spectrom.*, 1999, **14**, 621.
3 I. B. Gornushkin, B. W. Smith, H. Nasajpour and J. D. Winefordner, *Anal. Chem.*, 1999, **71**, 5157.
4 B. Walczak, B. van den Bogaert and D. L. Massart, *Anal. Chem.*, 1996, **68**, 1742.
5 I. Ruisanchez, P. Potokar, J. Zupan and V. Smolej, *J. Chem. Inf. Comp. Sci.*, 1996, **36**, 214.
6 J. I. Goldstein, D. E. Newbury, P. Echlin, C. Fiori, D. C. Joy and E. Lifshin, *Scanning Electron Microscopy and X-ray Microanalysis*, 2nd edn., Plenum Press, New York, 1981.
7 C.-J. Chin, C.-F. Wang and S.-L. Jeng, *J. Anal. At. Spectrom.*, 1999, **14**, 663.
8 D. W. Hahn, *Appl. Phys. Lett.*, 1998, **72**, 2960.
9 M. Saito, S. Izumida, K. Onishi and J. Akazawa, *J. Appl. Phys.*, 1999, **85**, 6353.
10 N. H. Cheung, C. W. Ng, W. F. Ho and E. S. Yeung, *Appl. Surf. Sci.*, 1998, **127–129**, 274.
11 R. J. Watling, B. F. Lynch and D. Herring, *J. Anal. At. Spectrom.*, 1997, **12**, 195.
12 L. A. Doyle, G. W. Martin, A. Al-Khateeb, I. Weaver, D. Riley, M. J. Lamb, T. Morrow and C. L. S. Lewis, *Appl. Surf. Sci.*, 1998, **127–129**, 716.
13 W. H. Press, B. P. Flannery, S. A. Teukolsky and W. T. Vetterling, *Numerical Recipes: the Art of Scientific Computing*, Cambridge University Press, New York, 1986, 381–453, 454–497.